

1 **Technical note: Detecting physically unrealistic outliers in ACE-FTSsatellite-**
2 **based atmospheric measurements**

3
4 P.E. Sheese¹, C.D. Boone², and K.A. Walker^{1,2}

5
6 ¹Department of Physics, University of Toronto, Toronto, ON, M5S 1A7, Canada

7 ²Department of Chemistry, University of Waterloo, Waterloo, ON, N2L 3G1, Canada

8 Corresponding author: K.A. Walker

9
10 **Abstract**

11 The ACE-FTS (Atmospheric Chemistry Experiment – Fourier Transform Spectrometer)
12 instrument on board the Canadian satellite SCISAT has been observing the Earth’s limb in
13 solar occultation since its launch in 2003. Since February 2004, high resolution (0.02 cm^{-1})
14 observations in the spectral region of $750\text{-}4400\text{ cm}^{-1}$ have been used to derive volume mixing
15 ratio profiles of over 30 atmospheric trace species and over 20 atmospheric isotopologues.
16 Although the full ACE-FTS level 2 data set is available to users in the general atmospheric
17 community, until now no quality flags have been assigned to the data ~~in order to guide the users~~.
18 This study describes the two-stage procedure for detecting physically unrealistic outliers within
19 the data set for each retrieved species, which is a fixed procedure across all species. Since the
20 distributions of ACE-FTS data across regions (altitude/latitude/season/local time) tend to be
21 asymmetric and multi-multimodal, the screening process does not make use of the median
22 absolute deviation. It makes use of volume mixing ratio probability density functions, assuming
23 that the data, when sufficiently binned, are at most tri-modal and that these modes can be

24 represented by the superposition of three normal, or log-normal, distributions. Quality flags have
25 been assigned to the data based on retrieval statistical fitting error, the physically unrealistic
26 outliers described in this study, and known instrumental/processing errors. The quality flags
27 defined and discussed in this study are now available for all level 2 versions 2.5 and 3.5 data and
28 will be made available as a standard product for future versions.

29

30 **Introduction**

31 One of the most common techniques for screening out anomalous data from a data set is
32 to calculate the set's mean (μ) and standard deviation (σ). Data that are outside the limits of $\mu \pm$
33 $k\sigma$, where k is some constant, are deemed to be outliers. Another common, and similar, method
34 is to use the median and MAD (Median Absolute Deviation) [*Leys et al., 2013; Toohey et al.,*
35 *2010; and references therein*], in place of the mean and standard deviation respectively, where,

$$\text{MAD} = \text{median}_i(|x_i - \text{median}_j(x_j)|). \quad (1)$$

36 This method is much less sensitive to extreme outliers, as the presence of outliers typically has
37 an insignificant effect on the median value. It can be used as an efficient tool in detecting outliers
38 for data that are normally distributed. However, ~~this technique assumes that~~ using this value as a
39 method of detecting outliers can be ineffective if the data being analyzed are not multi-
40 multimodal and/or are asymmetrically distributed about the median. In the case of data that ~~is~~ are
41 multimodal or asymmetrically ~~or multi-modally~~ distributed and ~~consists contain of~~ multiple
42 extreme outliers, it is likely that neither the σ nor the MAD will be an appropriate estimate of the
43 variation, or scale, of the measurements. In such cases, they should be avoided in the detection of
44 outliers [*Rousseeuw and Croux, 1993*].

45 In satellite remote sensing ~~of the atmospheric limb, measurements inherently suffer from~~

46 ~~sampling biases. Therefore~~, isolating geographical/seasonal/local time regions where global
47 satellite-based data are ~~normally-symmetrically~~ distributed and uni-modal can be difficult and/or
48 tedious. This is due to the fact that the atmosphere doesn't necessarily behave in a predictable,
49 periodic manner. Measurements grouped into a given altitude and latitude and month and local
50 time bin can be driven away from ~~typical~~normal behaviour by any number of factors— (e.g., the
51 polar vortex, a solar proton event, a sudden stratospheric warming, biomass burning, presence of
52 polar stratospheric clouds, etc.), thereby altering the “typical” distribution of observed
53 measurements, and hence the probability density function (pdf) of the trace species
54 concentration.

55 The often used method for detecting outliers of employing the MAD does not explicitly
56 make use of a pdf, but it does make the assumption the pdf is symmetric about the median value.
57 Other often used methods, such as Peirce's criterion [Peirce, 1852; Ross, 2003] and Chauvenet's
58 criterion [Chauvenet, 1871], explicitly make use of a pdf, however they assume that the pdf is a
59 Gaussian distribution. It should also be noted that in atmospheric science, the use of pdfs is not
60 uncommon in tracer and validation studies. Lary and Lait [2006], in their introduction, give
61 excellent examples of different types of tracer studies; and studies such as Migliorini et al.
62 [2004], Lary and Lait [2006], and Wu et al. [2008] have demonstrated that pdfs can be used as a
63 validation tool, where pdfs as measured by different atmospheric sounders are inter-compared
64 rather than inter-comparing co-located measurements.

65 The ACE-FTS (Atmospheric Chemistry Experiment – Fourier Transform Spectrometer
66 [Bernath et al., 2005]) instrument, on board the Canadian satellite SCISAT, is a solar
67 occultation, high spectral-resolution (0.02 cm^{-1}) Fourier transform spectrometer operating
68 between 750 and 4400 cm^{-1} . ACE-FTS observations are used to derive volume mixing ratio

69 (VMR) profiles of over 30 atmospheric trace gases, as well as profiles of over 20 subsidiary
70 isotopologues of atmospheric species [Boone *et al.*, 2005]. SCISAT was launched in 2003 and
71 ACE-FTS has been providing consistent measurements since February 2004. Atmospheric
72 profiles range in altitude from ~5-110 km, depending on the species, with a vertical resolution of
73 ~3-4 km and sampling of 12-6 km.

74 This study outlines the repercussions of screening data based on the ~~standard deviation~~
75 or the MAD given non-normally distributed data and discusses a two-step process for detecting
76 outliers that is currently carried out on the ACE-FTS level 2 data set. All data presented in this
77 study are ACE-FTS level 2 version 3.5 (v3.5) [Boone *et al.*, 2013] spanning February 2004 to
78 February 2013, however the same processes ~~have been~~ used for detecting outliers in version
79 2.5 (v2.5) data. The main differences in v3.5 from v2.5 are,

- 80 • Amended sets of microwindows for all molecules, and an increase in the number of
81 allowed interferers in the retrievals;
- 82 • Improvement in temperature/pressure retrievals, leading to a reduction in unphysical
83 oscillations in retrieved temperature profiles;
- 84 • Inclusion of COCl₂, COClF, H₂CO, CH₃OH, and HCFC-141b and removal of HOCl and
85 ClO VMR retrievals.

86 Physically unrealistic outliers can occur in the ACE-FTS level 2 for a number of different
87 reasons. Many of these are often caught prior to being added to the level 2 database, such as
88 outliers due to exceedingly noisy spectra, ice contamination affecting an occultation, and a
89 variety of processing errors. However, these aren't always caught by pre-screening, and other
90 factors, not accounted for in the pre-screening, can contribute to the presence of outliers, for
91 example, poor statistical fitting or convergence onto an unrealistic solution in the retrieval.

92 inaccurate pressure and temperature a priori information.

93 The outlier detection and subsequent data flagging procedures discussed in this study
94 have only been performed on the ACE-FTS level 2 data products that have been interpolated
95 onto a 1-km altitude grid (between 0.5 and 149.5 km) [Boone *et al.*, 2005]. The philosophical
96 approach for flagging-identifying data as potential outliers was one of caution, in that it is better
97 to keep some “bad” data (likely to be physically unrealistic) than to reject “good”, or “true”, data
98 (likely to be physically realistic).- ~~As well, it~~ was also desired that the approach be consistent for
99 all subsets of data being analyzed, i.e. tolerance levels, regional limits, etc. should be the same
100 for all species, for all seasons, at all altitudes. For the remainder of this study, these physically
101 unrealistic data will be referred to as “unnatural” outliers, and the data that are likely to be
102 physically realistic yet still seemingly outlying as “natural” outliers. All data that are not
103 unnatural outliers will be referred to as inliers.

104

105 **Detection method and results**

106 All distributions of data discussed in this section represent the February 2004-February
107 2013 data, and all VMRs are given in parts per volume (ppv).

108 Global satellite-based measurements of trace gases in the atmosphere typically are not
109 symmetrically normally distributed and are often multimodal. Different regions are governed by
110 different, varying processes, and therefore analysis of the data is typically carried out by
111 breaking down the data into different altitude, latitudinal, etc. bins. Figure 1 shows all the ACE-
112 FTS H₂O data at 17.5 and 35.5 km and the corresponding measurement distributions. For both
113 subsets of H₂O data, inlier limits were determined for $\mu \pm 3\sigma$ and $median \pm 3 MAD \times 1.428$
114 (1.428 is the scale factor for the MAD to equal the σ -consistent estimate of the variation

115 assuming a normal distribution [*Rousseeuw and Croux, 1993*]). These limits are plotted in Fig.
116 1a and Fig. 1c and highlight two key points: first, using the standard deviation when there are
117 extreme outliers can allow for the acceptance of data that ~~should clearly be rejected~~ are most
118 likely physically unrealistic. Second, using the MAD on multimodal or asymmetrically ~~or multi-~~
119 ~~modally~~ distributed data can lead to the rejection of physically realistic “good” data. For instance,
120 as shown in Fig. 1a, the lower cut-off using the MAD of 2.76 ppm clearly excludes the low H₂O
121 concentrations that are observed in Antarctic (austral) spring. As can be seen in Fig. 1b and Fig.
122 1d, the H₂O data at both altitude levels are not normally distributed.

123 The data can be separated further into bins based on latitudinal regions and local times.
124 For example, Fig. 2 shows H₂O and O₃ sunset data at 30.5 and 35.5 km, separated into different
125 latitude regions (0-30°S, 30-60°S, and 60-90°S), with dashed lines representing best fits to
126 ~~Gaussian~~ normal distributions. These regions are representative of bins often used to partition
127 atmospheric data. Figure 2 exemplifies that using a given bin definition that leads to data with a
128 symmetric and uni-modal distributions ~~symmetrically distributed data~~ at one altitude level doesn't
129 necessarily lead to a symmetric and uni-modal distribution of ~~symmetrically distributed~~ data at all
130 altitude levels, nor across all species. For instance, in Fig. 2a the 35.5 km O₃ distributions in all
131 three latitude regions are fairly symmetric. However the 35.5 km H₂O distribution, (Fig. 2c), in
132 the mid-latitudes is highly skewed, and in the high latitudes the distribution is tri-modal. ~~and in~~ In
133 Figs. 2b and d we see bimodal, asymmetric distributions for both O₃ and H₂O in the 30-60°S and
134 60-90°S regions at 30.5 km. For high-latitude data in many species' data sets, distributions can
135 be bimodal due to observing inside and outside of the vortex, and therefore it is not possible to
136 find sub-regions (based on season, latitude, or local time) that will always exhibit symmetric
137 distributions.

138 Therefore, the ACE-FTS data screening process takes an approach that does not require
139 the distribution of any subset of data to be symmetric or containing just one mode.

140 Initially, all data are pre-screened. Any occultation that contains errors due to previously
141 known issues (e.g. unrealistic N₂O concentrations due to a convergence failure for occultations
142 with low water levels, ice buildup on the detectors during early mission occultations, bad spectra
143 used in the calibration, level 0-1 processing errors, etc.) are removed prior to analysis. A full list
144 of known issues is given on the ACE validation website, <https://database.scisat.ca/validation>.
145 Then, for each species, at each altitude level, any data point with an absolute value greater than
146 10,000 times the median of all absolute values is rejected. Absolute values are used, as ACE-FTS
147 VMR retrievals are allowed to be negative, and therefore, in some cases the median of the actual
148 values could be very close to zero.

149 The screening processes starts by analysing the data's ~~probability density function~~pdfs.
150 The ~~normalized probability density function~~pdf of data subset x , $pdf(x)$, multiplied by the
151 number of data points, N , gives you the ~~expectation density function (edf)~~~~expected number of~~
152 ~~data points~~ at a given value of x ,

$$edfE(x) = N \times pdf(x). \quad (2)$$

153 The ~~total integral of function~~ ~~$E(x)$~~ is the ~~edf~~ is equal to N , and the integral between any two
154 ~~values of x~~ gives the number of expected data points within that range. For determining unnatural
155 ~~outliers, we want to find the values of x where the integral between infinity (negative and~~
156 ~~positive) and x_{lim} (lower and upper values) is less than 1.~~~~expectation distribution.~~ Anywhere that
157 the ~~integral (from infinity) of the edf~~~~expectation distribution~~ is less than 1 is most likely a
158 statistical outlier, as no data points are expected to be measured ~~beyond the~~~~at those~~ values of
159 ~~x_{lim}~~ , given the pdf . Therefore, the criterion for excluding data can be any value of x where

160 $\int_{-\infty}^x E(x')dx'$ or $\int_x^{\infty} E(x')dx'$ ~~$E(x)$~~ is less than or equal to 1. This is similar to Peirce's criterion
161 [*Peirce*, 1852; *Ross*, 2003] and Chauvenet's criterion [*Chauvenet*, 1871], which both assume a
162 normally distributed ~~probability density function~~pdf. The tolerance level can be varied to suit the
163 desired acceptance level of possible outliers. For ACE-FTS data, a tolerance level, determined
164 empirically, of 0.025×10^{-4} is used, which corresponds to a 97.599.99% confidence of an excluded
165 data point being an outlier—i.e., any value ~~x_{lim}~~ where $\int_{-\infty}^x E(x')dx' < 10^{-4}$ ~~or~~
166 $\int_x^{\infty} E(x')dx'$ is less than 0.025 is rejected.

167 This method, however, requires determining an analytical solution for the data's
168 ~~edf~~expectation distributions. For each of the 50+ ACE-FTS retrieved species, at each altitude
169 level, the data is separated into sunset and sunrise occultations, in order to separate into similar
170 local conditions, as well as into four different latitude regions: 60-90°S, 0-60°S, 0-60°N, and 60-
171 90°N. Due to the SCISAT orbital geometry, the majority of ACE-FTS measurements are at high
172 latitudes, and therefore each latitudinal bin has roughly the same number of profiles. The
173 distribution of each subset is then fit to a Gaussian mixed distribution, using three Gaussian
174 distributions. This assumes that the data is at most tri-modally distributed. Since it is not
175 uncommon for distributions of atmospheric measurements to be log-normal, the fit is done in
176 log-space. The fit is performed using the Matlab statistical toolbox, which uses an Estimation
177 Maximization algorithm [*McLachlan and Peel*, 2000]. In an effort to avoid fitting to extreme
178 outliers an ad-hoc "Olympic"-style method is employed, whereby the data set's five lowest and
179 five highest values are excluded in the fit. Figure 3 shows the O₃ distribution at 30.5 km in the
180 60-90°S and 60-90°N regions, along with the fitted ~~expectation distribution~~dfs and the three
181 Gaussian distributions derived in the fit for both cases. ~~It should be noted that prior to fitting a~~
182 ~~data subset to a Gaussian mixed distribution, profiles affected by previously determined issues~~

183 ~~either with the instrument or with the data processing have been excluded, and extreme outliers~~
184 ~~are screened out by assuming that any data points with absolute values greater than 10,000 times~~
185 ~~the median of the subset's absolute values are outliers.~~

186 Figure 4 shows three examples of ACE-FTS sunset data distributions—NO₂ at 60-90°S
187 and 30.5 km, CH₄ at 0-60°N and 17.5 km, and N₂O at 60-90°N and 20.5 km—and the
188 corresponding fitted ~~expectation distribution~~s. These were chosen in order to illustrate typical
189 results for commonly used ACE-FTS data. The average root-mean-square error (RMSE) between
190 the ~~expectation distribution~~s and actual distributions, over all species and data subsets, is 6%
191 and has a 1 σ deviation of 2%. ~~In the case of rare extreme events present in the data, which tend~~
192 ~~to be under-sampled in ACE-FTS data, the effect on the distribution can be to skew a tail end of~~
193 ~~the distribution, driving the shape of the tail away from Gaussian. An additional ad hoc method~~
194 ~~has been implemented to ensure that no “true” data is excluded in the screening process when~~
195 ~~rare extreme events occur that are not properly accounted for in the fit. For each subset, the~~
196 ~~standard deviation is calculated for the inlying data, where $E(x) > 10^{-4}$. This standard deviation~~
197 ~~we will call σ_{in} . Original upper and lower limiting values, x_t , are calculated, where $E(x_t) =$~~
198 ~~10^{-4} , and both the upper and lower limiting values are extended by σ_{in} . Hence, $x_{lim}^{up} = x_t^{up} +$~~
199 ~~σ_{in} and $x_{lim}^{low} = x_t^{low} + \sigma_{in}$.~~ Figure 5 shows the inliers and unnatural outliers as determined by
200 the ~~expectation distribution~~s for the subsets shown in Fig. 4. As can be seen, not all subsets
201 contain many extreme outliers, e.g. NO₂ at 30.5 km (Fig. 5a), which only has one detected
202 outlier. When there are obvious outliers, this method does exclude the most extreme outliers,
203 although perhaps not all unnatural outliers. For instance, several (potentially) anomalously low
204 values, near 0.75 ppm, in the CH₄ data (Fig. 5b) remain as inliers. This is in part due to the
205 relatively lax tolerance level of ~~10^{-4}~~ 0.025, which is more likely to leave in outliers than if a larger

206 value (but still less than 1) ~~were~~ chosen.

207 It should be noted that screening using the ~~expectation distribution~~ is a hard-limiting
208 filter. ~~Therefore, using it in the manner described above which~~ doesn't necessarily reject data
209 that are non-physically anomalous for a given season. To screen the data ~~of~~ for this type of
210 moderate outlier, the 15-day ~~running mean (μ_{15})~~ median and a 15-day ~~running standard deviation~~
211 (σ_{15}) variation scale are calculated for each subset, excluding outliers as determined from the
212 ~~expectation distributions~~. Even on a 15-day timescale, ACE-FTS subset data can have
213 distributions that are bimodal. In many cases, the primary mode is sampled much more
214 frequently than the secondary mode, and therefore, without careful consideration, data within the
215 secondary mode can be erroneously screened as unnatural outliers. To avoid this, we need a
216 variation scale that is sensitive to outliers (unlike the MAD), but not overly sensitive to outliers
217 (like the σ). For this we define a variation scale that is similar to the MAD, only more sensitive
218 to outliers—the MeAD,

$$\text{MeAD} = \text{mean}_i(|x_i - \text{median}_j(x_j)|). \quad (3)$$

219 Any data point with a value outside the bounds of ~~$\text{median}_{\mu_{15}} \pm 105.5 \times \sigma_{\text{MeAD}_{15}}$~~ are
220 considered to be unnatural outliers. The value of 105.5 was empirically found to maximize the
221 number of discovered unnatural outliers without rejecting obvious natural outliersly “true” data.
222 ~~If outliers are detected, they are removed from the data, and a new running mean and standard~~
223 ~~deviation are calculated for the inlying data in order to determine if there are any more outliers.~~
224 ~~This process is iterated until all data points are determined to be inliers. The mean and standard~~
225 ~~deviation are used instead of the median and MAD, as it is assumed that the subsets have already~~
226 ~~been screened for extreme outliers.~~ Figure 6 shows the inliers and outliers as determined by the
227 15-day running values for the subsets shown in Fig. 4. Clearly this step catches moderate outliers

228 that were not detected using the ~~expectation distribution~~df, although still not all anomalous data
229 have been screened out. The potentially anomalous values near 0.75 ppm in the CH₄ data (Fig.
230 6b) still remain as inliers. Stricter tolerance criteria in either the ~~expectation distribution~~df or
231 running ~~standard deviation~~MeAD screening process would allow for these data to be screened
232 out; however, they were found to lead to screening out “~~true~~” ~~data~~natural outliers in other subsets
233 of data, which would be discordant with our philosophical approach. Going back to the original
234 case of H₂O at 17.5 km (Fig. 1a), an example of the difference between using the MeAD as
235 opposed to the MAD in the second step is shown in Fig.7. However, now the focus is on only the
236 Antarctic data. The unnatural outliers and remaining inlying data for Antarctic H₂O at 17.5 km
237 are shown for the two different approaches. Fig.7a shows the results when using limiting values
238 of $median_{15} \pm 10 \times MeAD_{15}$, where the significant majority of the data points screened as
239 unnatural outliers are likely to be physically unrealistic for their local conditions. Using the
240 limiting values of $median_{15} \pm 10 \times MAD_{15}$, Fig. 7b, leads to many more outliers being
241 detected as unnatural outliers. Upon inspection, many of these erroneous “unnatural” outliers are
242 most likely being erroneously rejected, especially in late 2009 where ACE-FTS is most likely
243 routinely observing dehydrated air masses. In both cases, outliers were detected in the sunrise
244 and sunset data sets separately.

245 In order to explore the response to periodic extreme events and to trends, Fig. 87 shows
246 the final inliers and unnatural outliers in all ACE-FTS HCN data at 9.5 km, which exhibits
247 periodic increases that could correspond to biomass burning events [e.g. *Crutzen and Andreae,*
248 *1990; Pommrich et al., 2010*]; as well as all SF₆ data at 19.5 km, which exhibits a clear positive
249 trend throughout the time series [e.g. *Rinsland et al., 2005; Brown et al., 2011*]. Even in these
250 instances of extreme events and a significant trend in the data, the outlier detection method

251 outlined here is ~~able~~robust enough to keep the natural outliers~~data~~ as inliers. The top panels (a
252 and d) in Fig. 87 shows all data points and demonstrates the extreme unnatural outliers (red dots)
253 that can occur within the ACE-FTS data set. The middle panels (b and e) shows the same data as
254 the top panels, however without the more extreme unnatural outliers in order to better view the
255 data; and the bottom panels (c and f) shows the data with all unnatural outliers removed.

256 In the overwhelming majority of instances where the ACE-FTS VMR data exhibit a
257 sudden and/or extreme change in the distribution, the unnatural outlier detection method
258 described above does not screen out these events. Sudden stratospheric warmings cause there to
259 be strong descent in the northern high-latitude upper atmosphere. This leads to anomalously
260 large concentrations of NO_x and CO in the upper stratosphere-lower mesosphere, near 50 km [e.g.
261 *Manney et al.*, 2008; *Randall et al.*, 2009]. Figure 9a8 shows the time series of the final inliers
262 ~~and outliers~~ in all ACE-FTS NO_x and CO data at 55.5 km ~~and 50.5 km, respectively~~. It can be
263 seen that ~~Again~~, the detection method is robust enoughable to keep the majority of data during
264 these extreme events as inliers. Anderson et al. [2012], using in situ aircraft measurements,
265 demonstrated that in the summer there can be H₂O intrusions from the upper troposphere into the
266 lower stratosphere at Northern mid-latitudes. As can be seen in Fig. 9b, the final inlying ACE-
267 FTS data in the summer Northern mid-latitudes, in the lower stratosphere, do exhibit large
268 increases in H₂O concentrations. [Manney et al., 2011] showed that the Microwave Limb
269 Sounder (MLS) on the Aura satellite observes decreases in lower stratospheric HCl
270 concentrations in the Arctic vortex each spring; and in the spring of 2011, HCl concentrations
271 were anomalously low for a prolonged period. Figure 9c shows the final inlying ACE-FTS HCl
272 data in the Arctic, which are consistent with the MLS findings. No instances have been found in
273 which the unnatural outlier detection system outright rejects these types of phenomena. When

274 sudden, extreme changes do occur, the rejection of potential natural outliers has been minimized,
275 and the result of which is that the rejection of the detected unnatural outliers has an insignificant
276 effect on the mean. ~~In a couple extreme cases, NO data in early 2004 at 55.5 km (Fig. 8a-c),~~
277 ~~seven data points were flagged as extreme outliers that could potentially be “true” data; and~~
278 ~~similarly in early 2011 CO data at 50.5 km (Fig. 8d-f), eight data points may have been~~
279 ~~erroneously flagged. Out of all subsets of all 50+ species/isotopologues, these were the most~~
280 ~~extreme instances of apparent rejection of true data.~~ The disadvantageown side of not screening
281 out rare extreme events, however, is that this method is less likely to catch sporadic systematic
282 instrument or processing errors. Therefore, continual monitoring of both the rejected and non-
283 rejected data statistics is necessary to determine if any such errors have occurred.

284 Table 1 shows what percentage of ACE-FTS level 2 v3.5 profiles contain at least one
285 detected outlier (by either stepmethod). For any given species, if all profiles that contained at
286 least one outlier are rejected, less than 6% of the total number of profiles will be omitted.

287

288 **Conclusions**

289 A two-step process has been developed in order to screen all ACE-FTS level 2 data for
290 physically unrealistic outliers. The first step fits an ~~expectation distributiondf~~, the superposition
291 of three Gaussian distributions, to actual distributions. This fit is done in log-space. Data in the
292 tails of the distributions where the probability of finding a data point~~that have corresponding~~
293 ~~expectation values that are is~~ less than the ~~subset~~-tolerance level are determined to be extreme
294 unnatural outliers. The second step iteratively takes the 15-day running median and standard
295 deviationMeAD and screens for moderate seasonal unnatural outliers. ~~At each iteration, d~~Data
296 that are further than 105.5 times the MeADstandard deviation from the median are determined to

297 be moderate outliers.

298 Using these methods to screen the ACE-FTS data for unnatural outliers, a flagging
299 system has been implemented to give ACE-FTS level 2 data users a guide for how best to use the
300 data. Each VMR data point in each profile is flagged with an integer from 0-9. Table 2 gives the
301 definition for each flag value. Any data with a 0 flag ~~are~~^{is} recommended for use. In previous
302 versions, data users were recommended that they filter out data where the percent error (the
303 retrieval statistical fitting error divided by the retrieved value) is either greater than 100% or less
304 than 0.01%; for legacy reasons, these data have been given a flag value of 1. It is recommended
305 that data points with a corresponding flag greater than 2 be removed before any analysis is
306 performed. This screening method alone may be adequate when only looking at one altitude
307 level, however, profiles that contain an outlier at a given altitude level may also be compromised
308 at lower altitude levels. Therefore it is recommended that any profile that contains a flag between
309 4 and 7 (inclusive) be removed before analysis. ~~However, screening the data using these flags~~
310 ~~should be done with caution when investigating middle to upper atmospheric NO, CO, and CO~~
311 ~~isotopologues.~~

312 At certain altitude levels for a given species, the data can be either noisy, with a
313 significant number of negative values, or have a strong negative bias. In either case, since the
314 ACE-FTS retrieval allows for negative concentrations, it is possible for valid data to have values
315 close to zero, both positive and negative. When values are systematically near zero, the percent
316 error becomes extremely large. Therefore, in these situations, screening the data based on the
317 percent error may introduce a bias in the data. As such, before analysis, removing data that has a
318 corresponding flag value of 1 is only recommended at altitude levels where the overwhelming
319 majority of data points have a VMR value~~are~~ greater than zero.

320 Since the outlier detection methodology was approached with a philosophy that it is
321 better to leave in unnatural outliers than to remove natural outliers, there are outliers that have
322 gone un-flagged—especially in data sets that are inherently noisy and at low altitudes (below
323 ~10 km). Level 2 data users should use the defined quality flags as a starting point for screening
324 the data and be aware that some unnatural outliers may still exist that could be screened out prior
325 to analysis. ~~It is recommended that~~ data users ~~are also avoid~~ using the MAD in any attempts to
326 further screen the ACE-FTS level 2 data, for best results it is advised that they ensure that the
327 distribution of the data they are screening is not multimodal nor heavily skewed.

328 The flag values for all ~~v2.5, v3.0, and v3.5~~ are now available for download on the ACE-
329 FTS website, and v2.5 flag values ~~data~~ are available upon request from the lead author and will
330 soon be made available for download on the ACE-FTS website. It is currently expected that
331 similar flags will be a standard product within the level 2 data of all future products.

332

333 **Acknowledgements**

334 The authors wish to thank the anonymous referees for their comments and valuable
335 insight. This work was supported by the Canadian Space Agency (CSA). The Atmospheric
336 Chemistry Experiment is a Canadian-led mission mainly supported by the CSA.

337 **References**

- 338 Anderson, J. G., D. M. Wilmouth, J. B. Smith, and D. S. Sayres (2012), UV Dosage Levels in
339 Summer: Increased Risk of Ozone Loss from Convectively Injected Water Vapor, *Science*,
340 **337**, 835-839, doi:10.1126/science.1222978.
- 341 Bernath, P. F., C. T. McElroy, M. C. Abrams, C. D. Boone, M. Butler, C. Camy-Peyret, M.
342 Carleer, C. Clerbaux, P.-F. Coheur, R. Colin, P. DeCola, M. DeMazière, J. R. Drummond, D.
343 Dufour, W. F. J. Evans, H. Fast, D. Fussen, K. Gilbert, D. E. Jennings, E. J. Llewellyn, R. P.
344 Lowe, E. Mahieu, J. C. McConnell, M. McHugh, S. D. McLeod, R. Michaud, C. Midwinter,
345 R. Nassar, F. Nichitiu, C. Nowlan, C. P. Rinsland, Y. J. Rochon, N. Rowlands, K. Semeniuk,
346 P. Simon, R. Skelton, J. J. Sloan, M.-A. Soucy, K. Strong, P. Tremblay, D. Turnbull, K. A.
347 Walker, I. Walkty, D. A. Wardle, V. Wehrle, R. Zander, and J. Zou (2005), Atmospheric
348 Chemistry Experiment (ACE): Mission overview, *Geophys. Res. Lett.*, **32**, L15S01,
349 doi:10.1029/2005GL022386.
- 350 Boone, C. D., R. Nassar, K. A. Walker, Y. Rochon, S. D. McLeod, C. P. Rinsland, and P. F.
351 Bernath (2005), Retrievals for the Atmospheric Chemistry Experiment Fourier-Transform
352 Spectrometer, *Appl. Optics*, **44**, 7218-7231, doi:10.1364/AO.44.007218.
- 353 Boone, C. D., K. A. Walker, and P. F. Bernath (2013), Version 3 Retrievals for the Atmospheric
354 Chemistry Experiment Fourier Transform Spectrometer (ACE-FTS), The Atmospheric
355 Chemistry Experiment ACE at 10: A Solar Occultation Anthology, *A. Deepak Publishing*,
356 Hampton, Virginia, USA, pp. 103-127.
- 357 Brown, A. T., M. P. Chipperfield, C. D. Boone, C. Wilson, K. A. Walker, and P. F. Bernath
358 (2011), Trends in atmospheric halogen containing gases since 2004, *J. Quant. Spectrosc.*
359 *Rad. Trans.* **112**, 2552-2566, doi:10.1016/j.jqsrt.2011.07.005.

360 Chauvenet, W. (1871), Manual of spherical and practical astronomy, *J. B. Lippincott Company*,
361 Philadelphia, USA, pp. 558-563.

362 Crutzen, P. J., and M. O. Andreae (1990), Biomass burning in the tropics: impact on atmospheric
363 chemistry and biogeochemical cycles, *Science*, **250**, 1669–1678,
364 doi:10.1126/science.250.4988.1669.

365 Lary, D. J. and L. Lait (2006), Using probability distribution functions for satellite validation,
366 *IEEE Trans. Geosci. Remote Sens.*, **44**, 1359–1366, doi:10.1109/TGRS.2005.860662.

367 Leys, C., C. Ley, O. Klein, P. Bernard, and L. Licata (2013), Detecting outliers: Do not use
368 standard deviation around the mean, use absolute deviation around the median, *J. Exp. Soc.*
369 *Psychol.*, **49**, 764–766, doi:10.1016/j.jesp.2013.03.013.

370 Manney, G. L., W. H. Daffer, K. B. Strawbridge, K. A. Walker, C. D. Boone, P. F. Bernath, T.
371 Kerzenmacher, M. J. Schwartz, K. Strong, R. J. Sica, K. Krüger, H. C. Pumphrey, A.
372 Lambert, M. L. Santee, N. J Livesey, E. E. Remsberg, M. G. Mlynczak, and J. R. Russell III
373 (2008), The high Arctic in extreme winters: vortex, temperature, and MLS and ACE-FTS
374 trace gas evolution, *Atmos. Chem. Phys.*, **8**, 505-522, doi:10.5194/acp-8-505-2008.

375 Manney, G. L., M. L. Santee, M. Rex, N. J. Livesey, M. C. Pitts, P. Veefkind, E. R. Nash, I.
376 Wohltmann, R. Lehmann, L. Froidevaux, L. R. Poole, M. R. Schoeberl, D. P. Haffner, J.
377 Davies, V. Dorokhov, H. Gernandt, B. Johnson, R. Kivi, E. Kyrö, N. Larsen, P. F. Levelt, A.
378 Makshtas, C. T. McElroy, H. Nakajima, M. C. Parrondo, D. W. Tarasick, P. von der Gathen,
379 K. A. Walker, and N. S. Zinoviev (2011), Unprecedented Arctic ozone loss in 2011, *Nature*,
380 **478**, 469-U65, doi:10.1038/nature10556.

381 McLachlan, G., and D. Peel (2000), Finite Mixture Models, *John Wiley & Sons, Inc.*, Hoboken,
382 New Jersey, USA.

383 [Migliorini, S., C. Piccolo, and C. D. Rodgers, C. D \(2004\), Intercomparison of direct and indirect](#)
384 [measurements: Michelson Interferometer for Passive Atmospheric Sounding \(MIPAS\) versus](#)
385 [sonde ozone profiles, J. Geophys. Res., 109, D19316, doi:10.1029/2004JD004988.](#)

386 Peirce, B. (1852), Criterion for the rejection of doubtful observations, *Astronomical J.*, **2**, 161-
387 163.

388 Pommrich, R., R. Müller, J.-U. Grooß, G. Günther, P. Konopka, M. Riese, A. Heil, M. Schultz,
389 H.-C. Pumphrey, and K.A. Walker (2010), What causes the irregular cycle of the
390 atmospheric tape recorder signal in HCN?, *Geophys. Res. Lett.* **37**, L16805,
391 doi:10.1029/2010GL044056.

392 Randall, C. E., V. L. Harvey, D. E. Siskind, J. France, P. F. Bernath, C. D. Boone, and K. A.
393 Walker (2009), NO_x descent in the Arctic middle atmosphere in early 2009, *Geophys. Res.*
394 *Lett.*, **36**, L18811, doi:10.1029/2009GL039706.

395 Rinsland, C. P., C. Boone, R. Nassar, K. Walker, P. Bernath, E. Mahieu, R. Zander, J. C.
396 McConnell, and L. Chiou (2005), Trends of HF, HCl, CCl₂F₂, CCl₃F, CHClF₂ (HCFC-22),
397 and SF₆ in the lower stratosphere from Atmospheric Chemistry Experiment (ACE) and
398 Atmospheric Trace Molecule Spectroscopy (ATMOS) measurements near 30°N latitude,
399 *Geophys. Res. Lett.*, **32**, L16S03, doi:10.1029/2005GL022415.

400 Ross, S. M. (2003), Peirce's criterion for the elimination of suspect experimental data, *J. Eng.*
401 *Tech.*, **20**, 38-41.

402 Rousseeuw, P. J., and C. Croux (1993), Alternatives to the Median Absolute Deviation, *J. Amer.*
403 *Stat. Assoc.*, **88**, 1273-1283.

404 Toohey, M., K. Strong, P. F. Bernath, C. D. Boone, K. A. Walker, A. I. Jonsson, and T. G.
405 Shepherd (2010), Validating the reported random errors of ACE-FTS measurements. *J.*

406 *Geophys. Res.*, **115**, D20304, doi:10.1029/2010JD014185.

407 Wu, D. L., J. H. Jiang, W. G. Read, R. T. Austin, C. P. Davis, A. Lambert, G. L. Stephens, D. G.

408 Vane, and J. W. Waters (2008), Validation of the Aura MLS cloud ice water content

409 measurements, *J. Geophys. Res.*, **113**, D15S10, doi:10.1029/2007JD008931.

410

411 **Tables**

412 Table 1 – Percent rejection of ACE-FTS level 2 v3.5 profiles that contain one or more detected
 413 unnatural outlier (either by running MeADmean or expectation distributiondf).

Species	% reject	Species	% reject	Species	% reject
C ₂ H ₂	1.5471	HCFC141b	1.822.03	C ¹⁷ O	1.9567
C ₂ H ₆	1.891	HCFC142b	1.6681	C ¹⁸ O	2.5421
CCl ₂ F ₂	2.1009	HCl	2.189	O ¹³ CO	4.463.98
CCl ₃ F	1.5366	HCN	2.2650	O ¹³ C ¹⁸ O	1.3009
CCl ₄	1.6781	HCOOH	1.952.09	OC ¹⁷ O	1.3324
CF ₄	1.832.35	HF	1.4653	OC ¹⁸ O	4.9059
CFC113	1.3350	HNO ₃	2.2565	H ¹⁷ OH	2.9574
CH ₃ Cl	2.1139	HNO ₄	2.349	H ¹⁸ OH	3.082.91
CH ₃ OH	2.4083	N ₂	2.0862	HDO	2.7670
CH ₄	2.8195	N ₂ O	3.964.29	¹⁵ NNO	2.3928
CHF ₂ Cl	2.2935	N ₂ O ₅	2.156	N ¹⁵ NO	2.3734
ClONO ₂	1.768	NO	4.5091	NN ¹⁷ O	1.8877
CO	4.0310	NO ₂	2.2234	NN ¹⁸ O	2.9194
CO ₂	5.3970	O ₂	1.812.23	O ¹⁷ OO	3.032.98
COCl ₂	2.0837	O ₃	2.2440	O ¹⁸ OO	1.9795
COCIF	1.2935	OCS	1.452	OO ¹⁸ O	1.8573
COF ₂	1.3126	SF ₆	2.252.31	O ¹³ CS	2.1720
H ₂ CO	3.043	¹³ CH ₄	3.002.98	OC ³⁴ S	1.922.04
H ₂ O	3.8197	CH ₃ D	2.012.17		
H ₂ O ₂	2.743.16	¹³ CO	3.082.94		

414

415 Table 2 – Definition of flag values associated with ACE-FTS level 2 data

416

Flag value	Definition
0	No known issues with data
1	Percent error is not within 0.01-100%, and no other category of flag applies
2	Not enough data points in the region to do statistical analysis, and percent error is within 0.01-100%
3	Not enough data points in the region to do statistical analysis, and percent error is not within 0.01-100%
4	Moderate <u>unnatural</u> outlier detected from running <u>MeADmean</u> , percent error within limits
5	Extreme <u>unnatural</u> outlier detected from expectation-distribution <u>df</u> , percent error within limits
6	<u>Unnatural</u> Θ outlier detected and percent error is outside of limits
7	Instrument or processing error
8	Error fill value of -888 (data is scaled a priori)
9	Data fill value of -999 (no data)

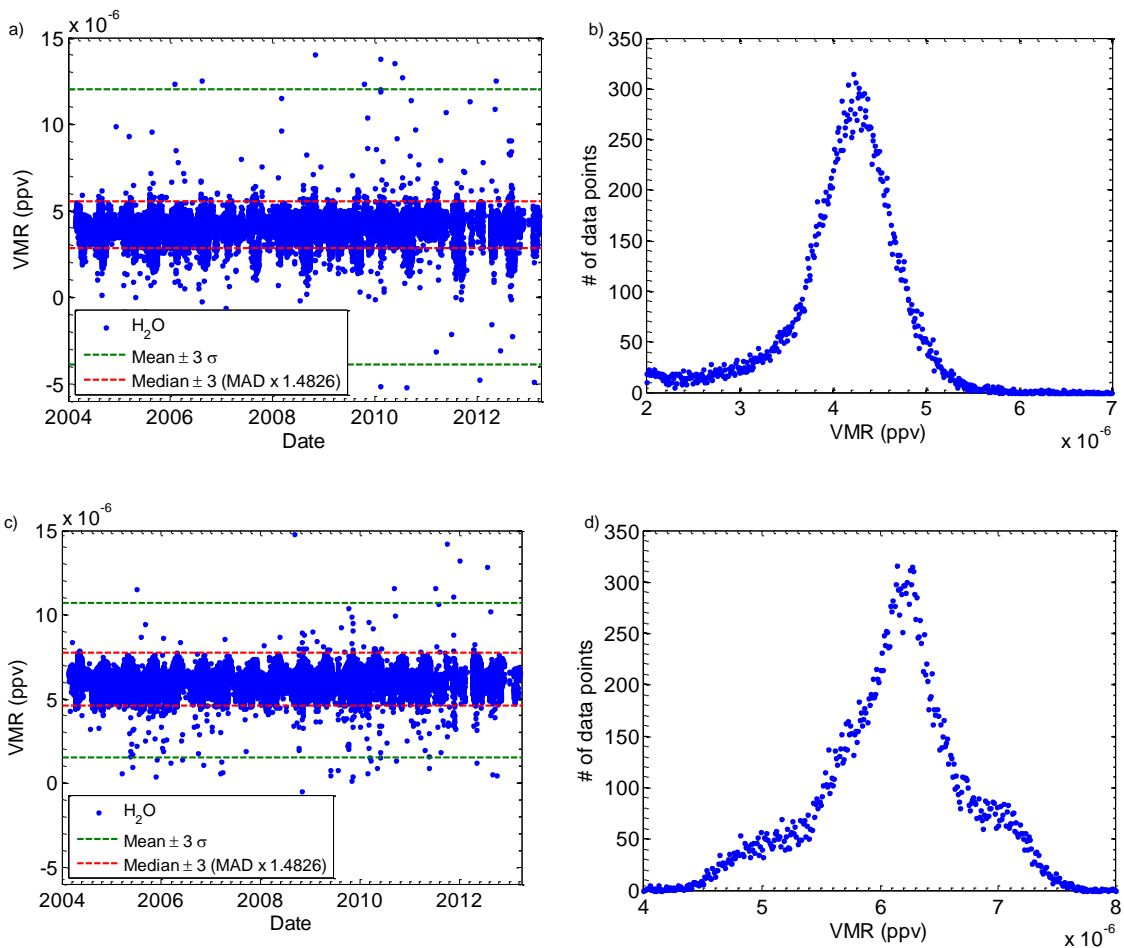
417

418 **Figures**

419

420 Fig. 1 – ACE-FTS level 2 v3.5 H₂O data (left) and corresponding distributions (right). Top panel

421 shows all data at 17.5 km, and the bottom panel shows all data at 35.5 km.

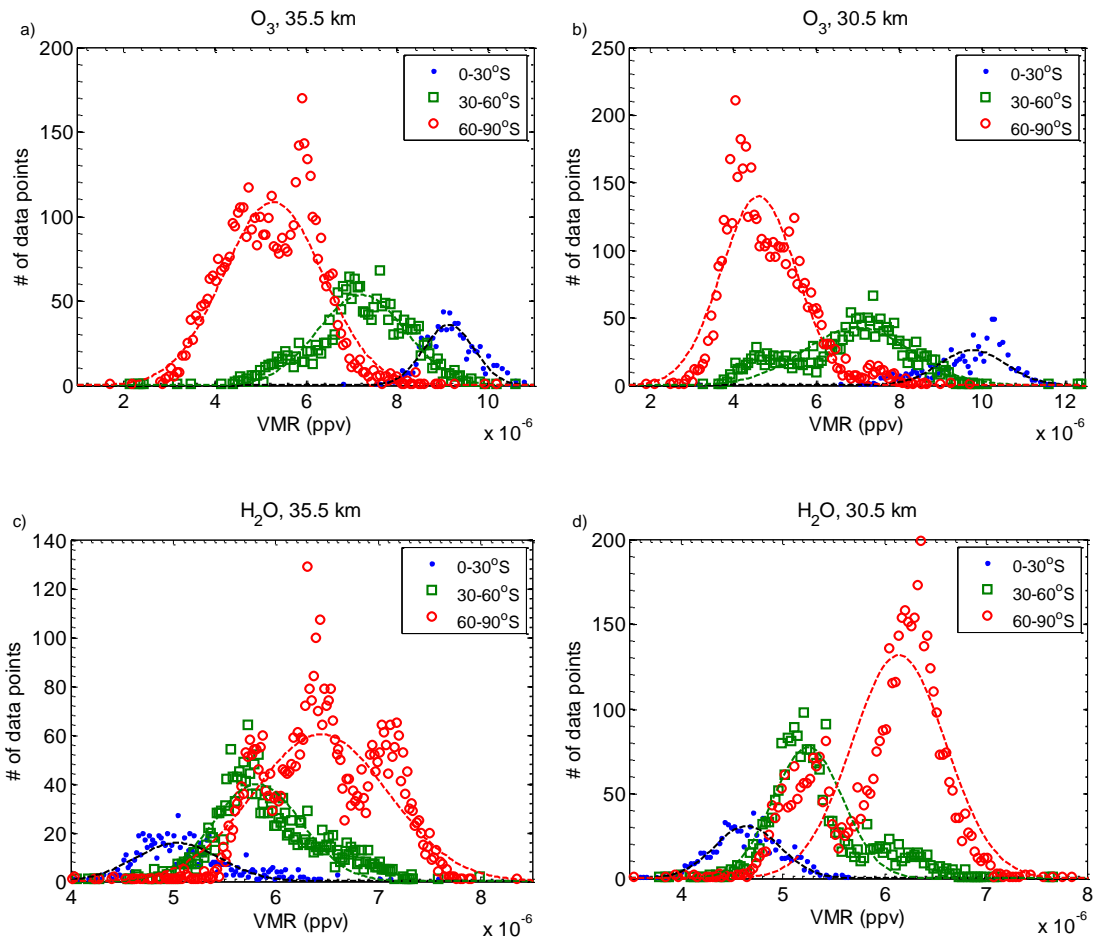


422

423

424

425 Fig. 2 – 2004-2013 ACE-FTS VMR distributions for sunset occultations (symbols) in the
426 Southern hemisphere and corresponding best fits to normal distribution (dashed lines). (a) O₃ at
427 35.5 km, (b) O₃ at 30.5 km, (c) H₂O at 35.5 km, (d) H₂O at 30.5 km.

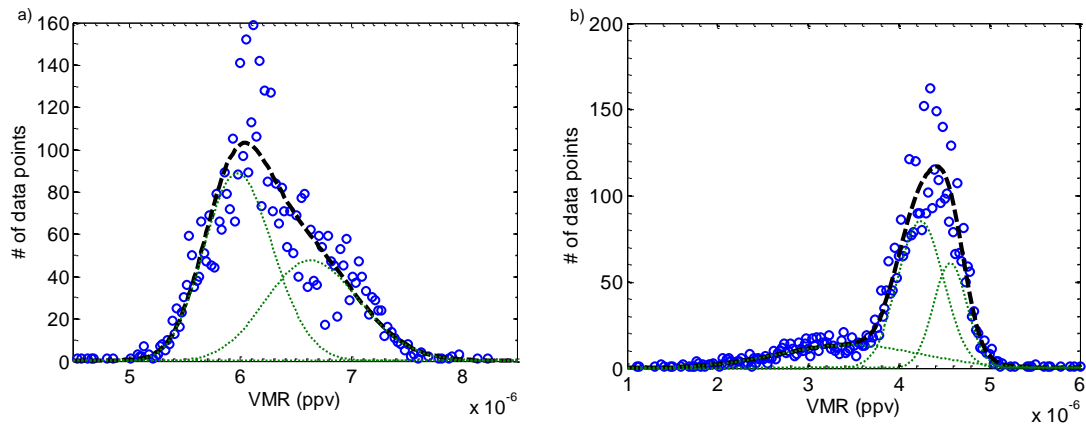


428

429

430

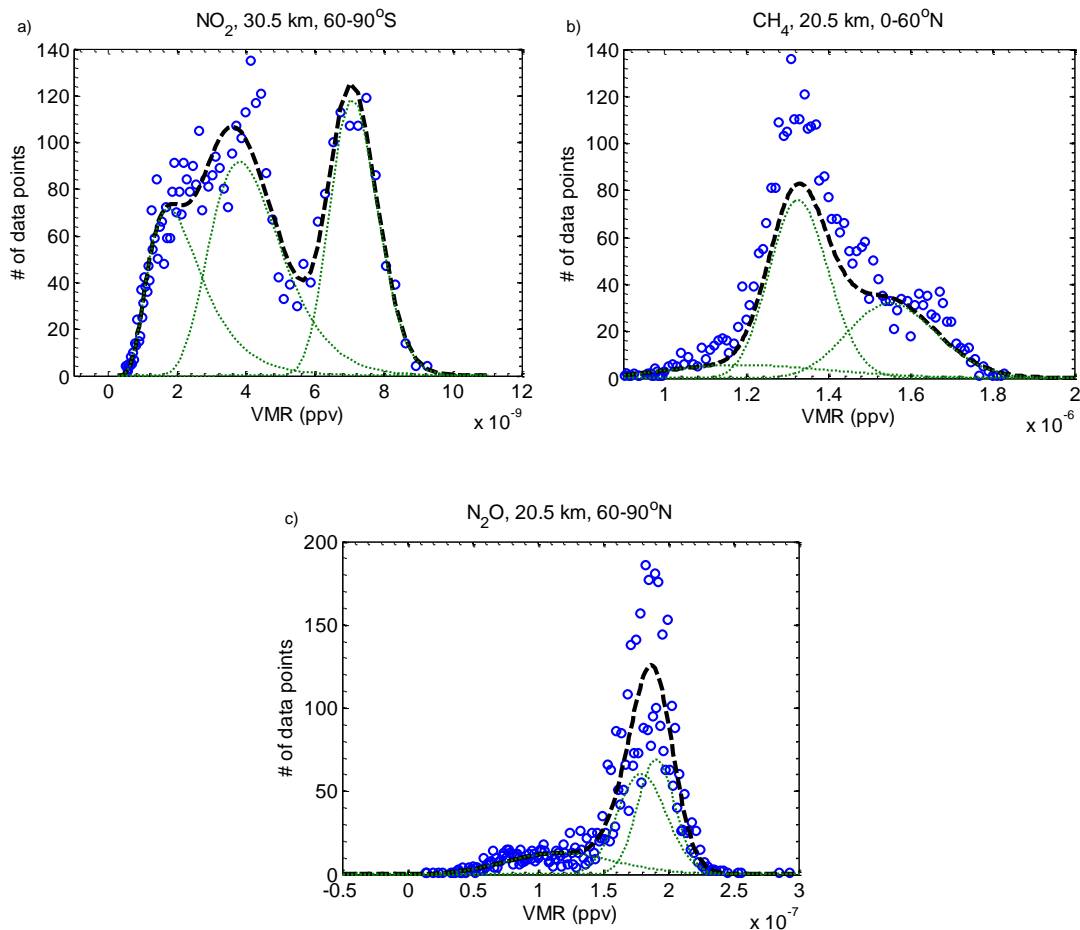
431 Fig. 3 – Sunrise ACE-FTS O₃ VMR distributions at 30.5 km (blue circles) and fitted ~~expectation~~
432 ~~distributions~~ (dashed black lines) for (a) 60-90°N, and (b) 60-90°S. Dotted green lines are the
433 fitted Gaussian distributions in calculating each of the expectation distributions, and the fitted
434 distributions have been normalized to the measured VMR distributions.



435

436

437 Fig. 4 – Sunrise ACE-FTS VMR distributions (blue circles) and fitted ~~expectation distribution~~dfs
 438 (black dashed lines) for (a) NO₂ at 30.5 km in the latitude region 60-90°S; (b) CH₄ at 20.5 km, 0-
 439 60°N; and (c) N₂O at 20.5 km, 60-90°N. Dotted green lines are the fitted Gaussian distributions
 440 in calculating each of the edfs, and the fitted distributions have been normalized to the measured
 441 VMR distributions.

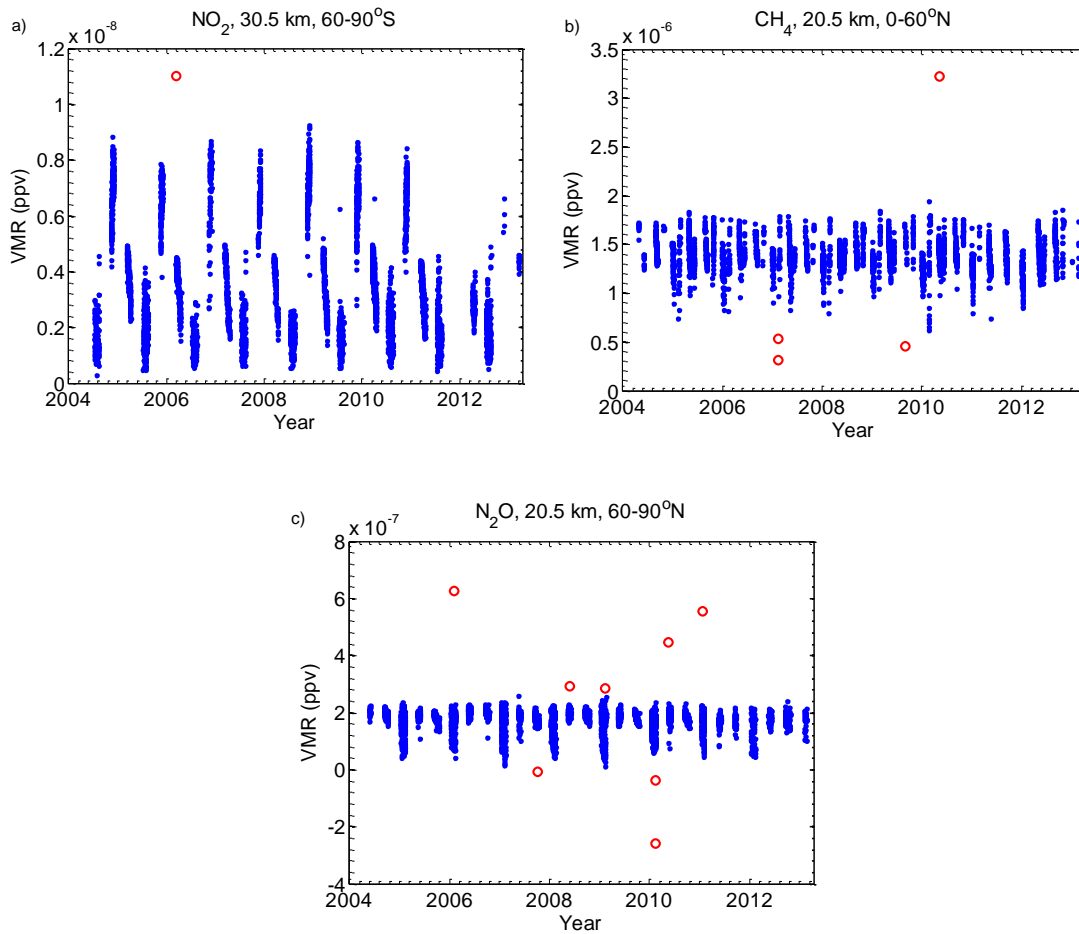


442

443

444

445 Fig. 5 – Sunrise ACE-FTS data for the same data subsets as Fig. 4. Red circles are data that have
446 been determined to be unnatural outliers outlying data as per the expectation distribution dfs, and
447 blue dots are the inlying data.

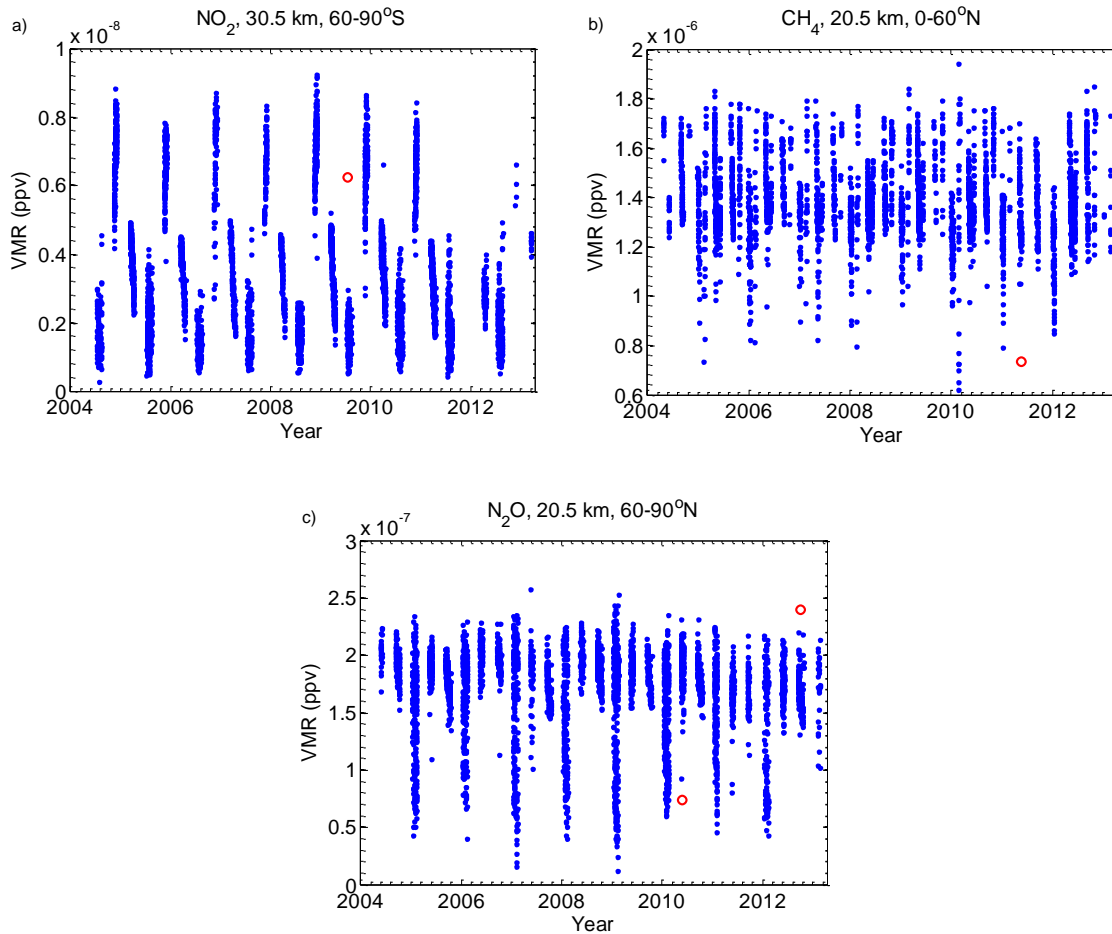


448

449

450

451 Fig. 6 – Sunrise ACE-FTS data for the same data subsets as Fig. 4. Red circles are data that have
452 been determined to be unnatural outliers-outlying data as per the 15-day running median and
453 MeADstandard-deviation, and blue dots are data that have been determined to be inliers.



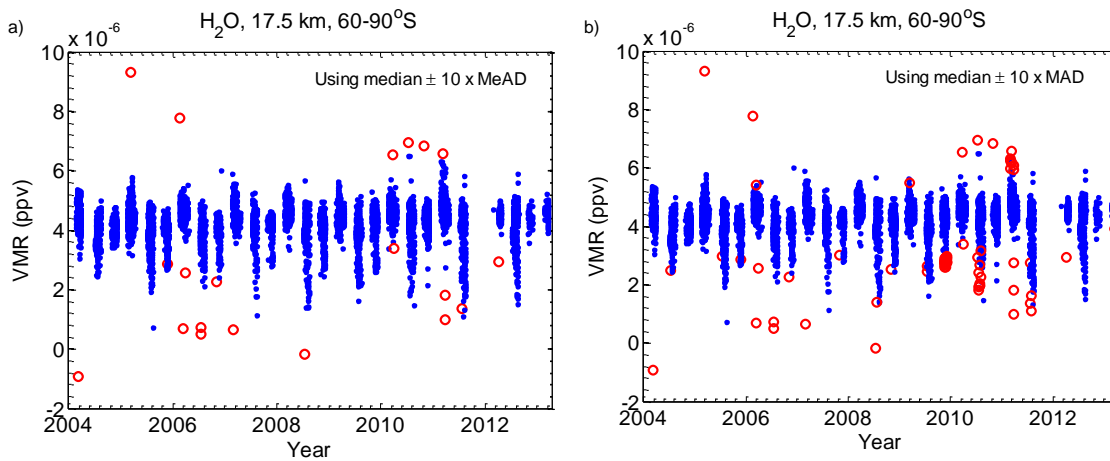
454

455

456

457 Fig. 7 – All Antarctic ACE-FTS data for H₂O at 17.5 km. Red circles are data that have been
458 determined to be unnatural outliers following two different methods (sunrise and sunset data
459 were analyzed separately), and blue dots are data that have been determined to be inliers. (a)
460 Unnatural outliers determined using the 15-day running MeAD, (b) Unnatural outliers
461 determined using the 15-day running MAD. Unnatural outliers as determined by the edfs are not
462 shown and were not used in the analysis.

463

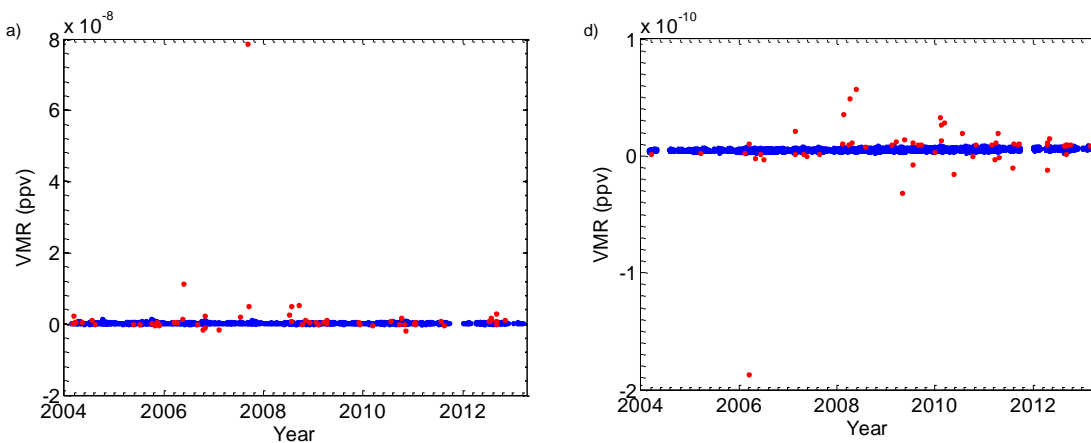


464

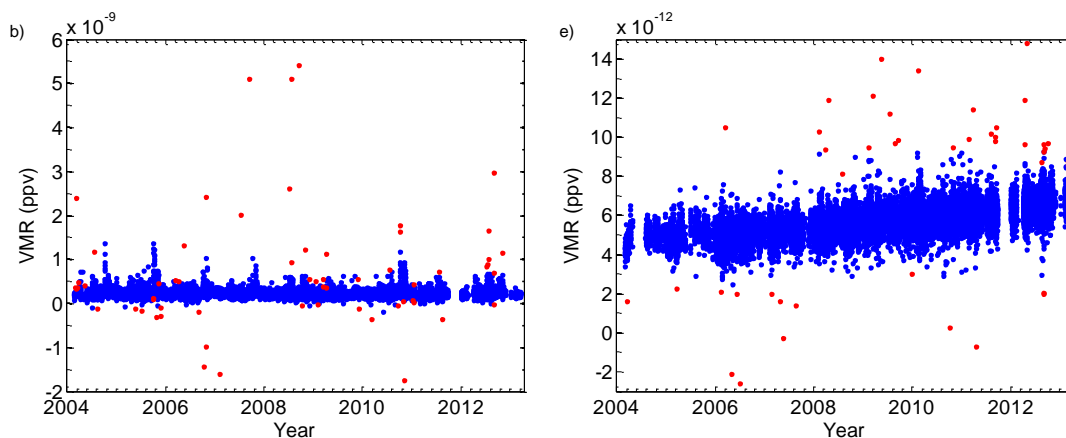
465

466 Fig. 87 – The final inlying data (blue dots) and unnatural outliers (red dots) ~~data~~ for all
467 ACE-FTS HCN data at 9.5 km (left) and SF₆ data at 19.5 km (right). The top panel shows all
468 data, the middle panel is the same as the top panel only zoomed in for clarity, and the bottom
469 panel is all data excluding the unnatural outliers.

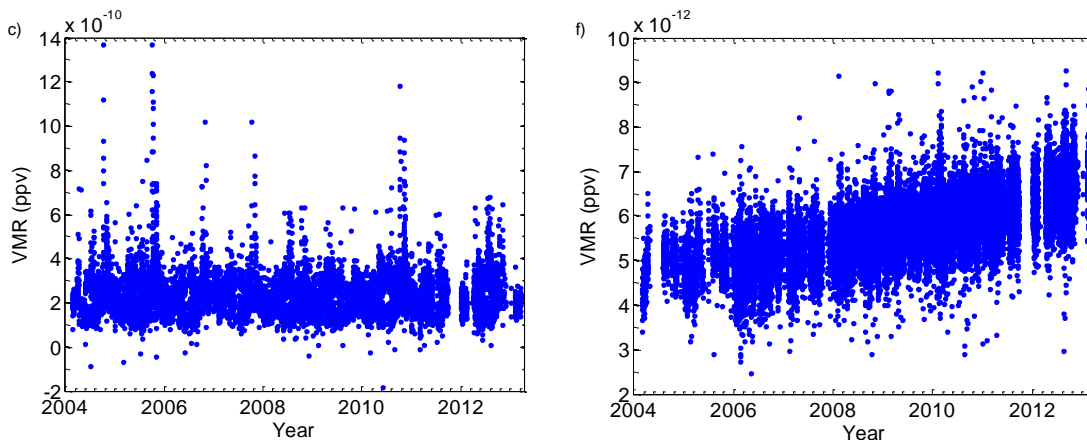
470



471

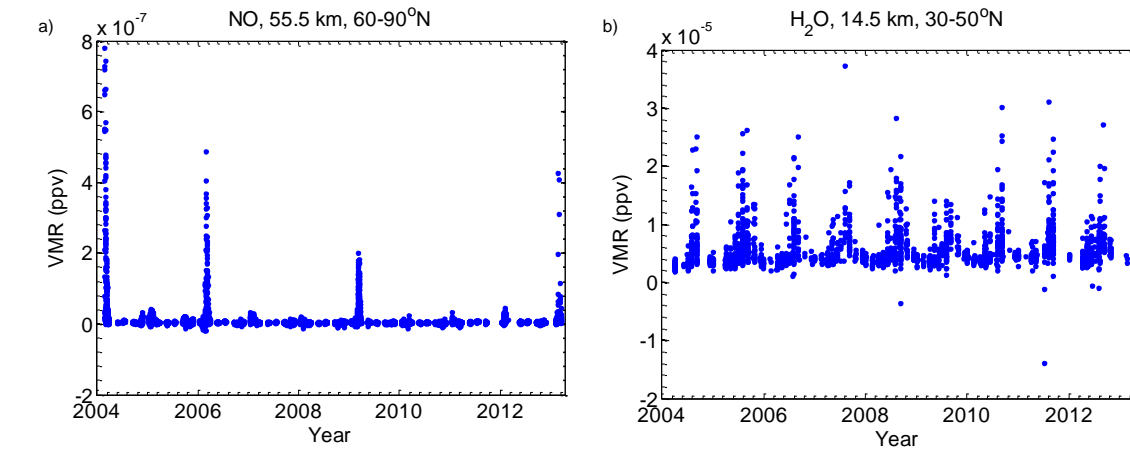


472

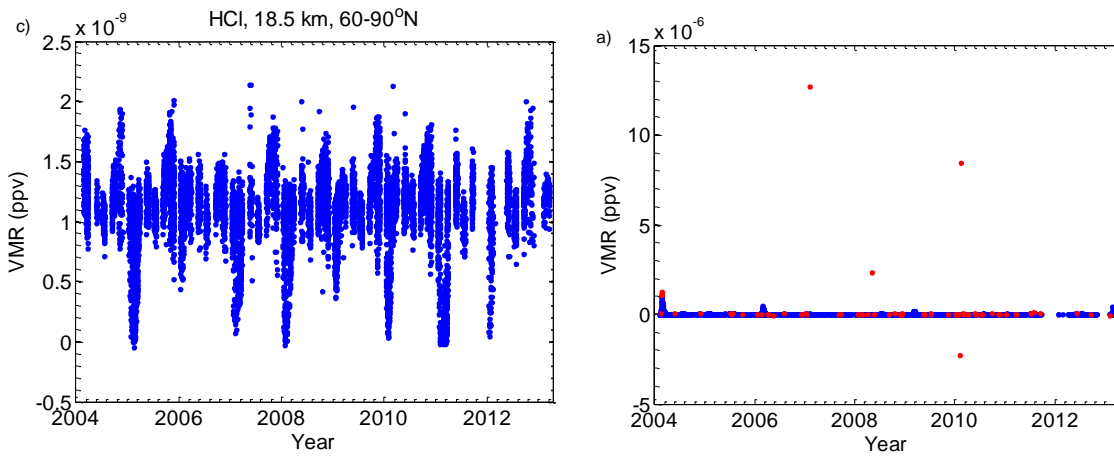


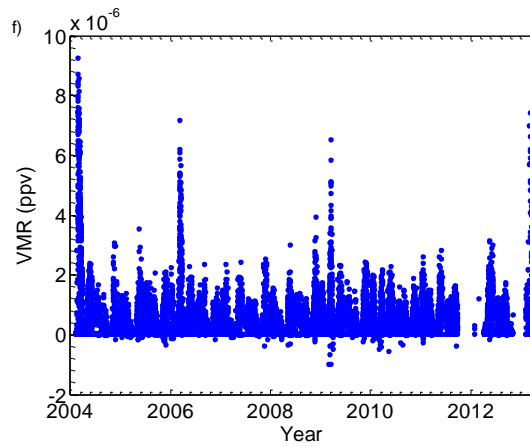
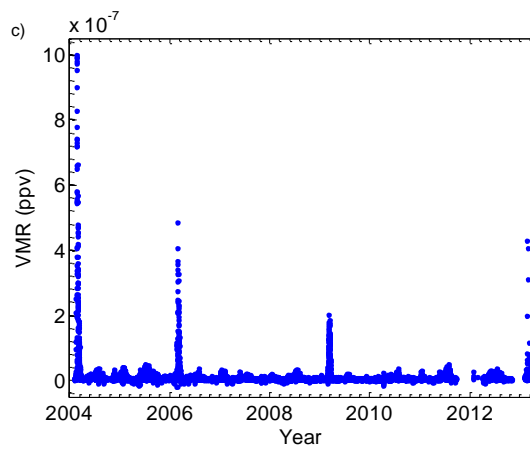
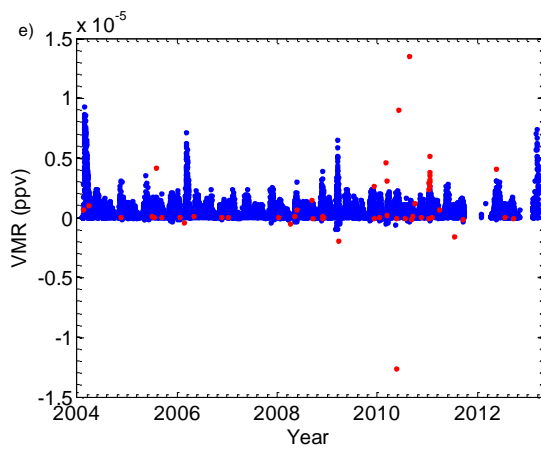
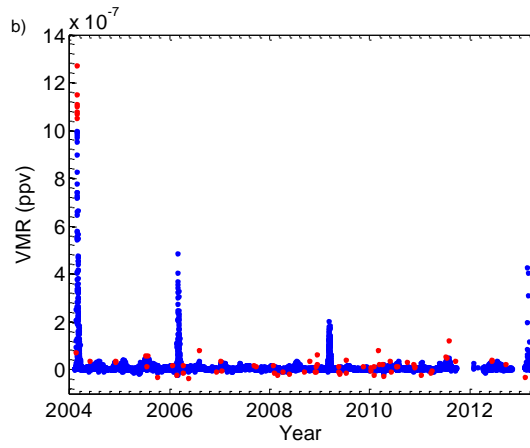
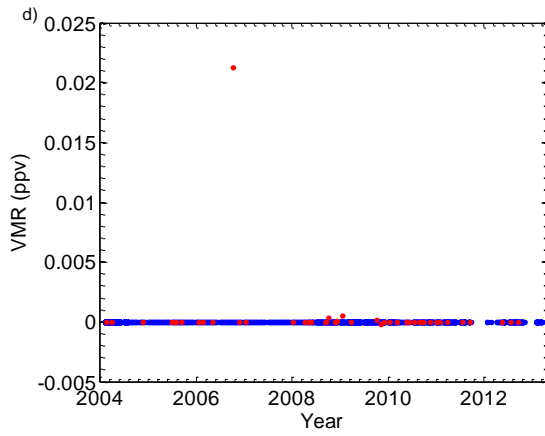
473 Fig. 98 – The final inlying data for (blue dots) and outlying (red dots) data for all ACE-FTS (a)
474 Arctic NO data at 55.5 km, (bleft) mid-latitude and COH₂O data at 1450.5 km, and (cright)
475 Arctic HCl at 18.5 km. The top panel shows all data, the middle panel is the same as the top
476 panel only zoomed in for clarity, and the bottom panel is all data excluding the outliers.

477



478





479

480

481

482